Agri 2024;36(1):1–12
doi: 10.14744/agri.2022.97957

ORIGINAL ARTICLE

Effects of continuous and pulsed radiofrequency applied for 120 and 240 seconds to rats' sciatic nerve

Rat siyatik sinirine 120 ve 240 saniye olarak uygulanan devamlı ve pulsed radyofrekansın etkileri

Güray ÖZKUMUR,[1] Esma KIRIMLIOĞLU,[2] Ergi KAYA,[3] Necdet DEMİR,[2] Mehmet Arif YEĞİN[1]

Summary

Objectives: Radiofrequency (RF) has been used for many years for pain treatment. The effects of RF on nerves and the underlying mechanism of these effects are not clearly understood. The aim of this study is to show the effects of Pulsed (P-RF) and Continuous (C-RF) RF in light and electron microscopy, and to determine the differences between them.

Methods: In this study, a total of 60 Rattus norvegicus rats were used in 6 groups. No procedure was performed on the control group. In the Sham group, the electrodes were placed but no current was applied. P-RF for 120 seconds, P-RF for 240 seconds, C-RF for 120 seconds, and C-RF for 240 seconds at 42 °C were applied respectively to the other groups. Sections obtained from sciatic nerves were examined with light and electron microscopy.

Results: Examinations of the Sham, P120, and C120 groups were normal. In P240, some morphological changes were observed, but when all samples were examined, these abnormalities were evaluated as negligible. In C240, severe deformation of both myelinated and non-myelinated nerve fibers was observed under an electron and light microscope. Dramatic structural deformities in Schwann cells were observed.

Conclusion: P120, P240, and C120 treatments did not produce any deformities in the sciatic nerve. The application of C-RF for 240 seconds produced pathological alterations in the nerve structure.

Keywords: Continuous radiofrequency; histological effects; pulsed radiofrequency; sciatic nerve.

Özet

Amaç: Radyofrekans (RF) ağrı tedavisi için yıllardır kullanılmaktadır. RF'in sinirler üzerindeki etkisi ve etki mekanizması halen net olarak ortaya konulmamıştır. Bu çalışmanın amacı; Pulsed RF (P-RF) ve Devamlı RF (C-RF)'nin oluşturduğu etkiyi ışık ve elektron mikroskobisi aracılığıyla incelemek ve farklılıklarını ortaya koymaktır.

Gereç ve Yöntem: Bu çalışmada 60 adet Rattus Norvegicus cinsi rat 6 gruba ayrılarak kullanılmıştır. Kontrol grubu alınmamıştır. Sham grubunda elektrotlar yerleştirilmiş ancak akım uygulanmamıştır. P-RF 120 saniye (sn), P-RF 240 sn, C-RF 120 sn, C-RF 240 sn, 42 ˚C'de diğer gruplara uygulanmıştır. Siyatik sinir kesitleri alınmış, ışık ve elektron mikroskopunda incelenmiştir.

Bulgular: Sham, P120 ve C120 grupları normal sınırlarda tespit edilmiştir. P240 grubunda bir takım morfolojik değişiklikler izlense de bütün örnekler incelendiğinde bu durumun ihmal edilebilir olduğu sonucuna varılmıştır. C240 grubunda ise hem miyelinli hem de miyelinsiz sinir liflerinde, ışık ve elektron mikroskopunda ağır deformasyon izlenmiştir. Schwann hücrelerinde dramatik yapısal bozukluklar gözlemlenmiştir.

Sonuç: P120, P240 ve C120 tedavileri siyatik sinirde herhangi bir deformiteye yol açmamıştır. C-RF 240 saniye uygulanması ise sinir yapısında patolojik değişikliklere yol açmaktadır.

Anahtar sözcükler: Devamlı radyofrekans; histolojik etkiler; pulsed radyofrekans; siyatik sinir.

Introduction

Pain is a subjective feeling of discomfort which is seen as a symptom of many diseases. According to the International Association for the Study of Pain (IASP), the definition of pain is "an unpleasant sensory and emotional experience associated with actual or potential tissue damage or described in terms of such damage".[1]

[1]Department of Anesthesiology and Reanimation, Akdeniz University Faculty of Medicine, Antalya, Türkiye
[2]Department of Histology and Embryology, Akdeniz University Faculty of Medicine, Antalya, Türkiye
[3]Department of Neurology, Dokuz Eylül University Faculty of Medicine, İzmir, Türkiye

Submitted ***(Başvuru):*** **06.01.2022** **Revised** ***(Revize):*** **19.09.2022** **Accepted** ***(Kabul):*** **24.10.2022** **Available online** ***(Online yayımlanma):*** **21.12.2023**

Correspondence: Dr. Mehmet Arif Yeğin. Akdeniz Üniversitesi Tıp Fakültesi, Anesteziyoloji ve Reanimasyon Anabilim Dalı, Antalya, Türkiye.
Phone: +90 - 242 - 249 60 00 **e-mail:** ayegin@akdeniz.edu.tr

Pain management is complex and requires a multidisciplinary approach. There are different biomedical and biopsychosocial ways of preventing pain. Biomedical pathways can be classified as pharmaceutical, electrical, and surgical or invasive and noninvasive methods.[2] Radiofrequency ablation (RF) is a safe and effective invasive method.[3,4] It has been successfully applied in different regions for a long time.[5–9] Nowadays, RFA is applied in two procedures, Conventional (C-RF) and Pulsed Radiofrequency (P-RF).

The C-RF technique is older and causes more heat complications. In the C-RF technique, the cannula is placed parallel to the nerve, and the current is continuous. The produced current leads to generating heat and an electromagnetic field. Application time and heat differ according to nerves and procedures. C-RF causes coagulation necrosis in nerves. It has very destructive effects on the nerves. C-RF is a painful procedure, so it is practiced with anesthesia. In the P-RF technique, the cannula is placed perpendicular to the nerve, and the current is not continuous. The produced current gives rise to an electrical field. Thus, heat complications are reduced. And since P-RF is a painless procedure, there is no need for anesthesia.[10–12] On the other hand, RF can cause neurodegenerative effects on the nerve. Erdine et al.[13] investigated the effect of RF in rabbits. They found RF can cause ultrastructural changes and P-RF is less destructive than C-RF. For rats, few studies compare the morphological effects of P-RF and C-RF. In these studies, researchers determined that P-RF was less destructive than C-RF. According to this study, both P-RF and C-RF can cause morphological changes in nerve tissue in rats.[14–16]

Pain management must be harmless and effective. The P-RF technique comes forward in pain treatment because it has fewer side effects and does not require anesthesia. However, there is no consensus on the morphological effects of P-RF and C-RF treatment. In addition, no studies are comparing the effects of RF application time on nerve morphology.

This study aimed to determine the ultrastructural changes of P-RF/CRF therapy and to determine whether different application times would cause different ultrastructural changes in the sciatic nerves of rats.

Table 1. Groups of rats

Group	N	Process	Tem.	Time (sec)
Control	10	–	–	–
Sham	10	Just electrode, no radiofrequency	–	–
P120	10	P-RF	42 °C	120
P240	10	P-RF	42 °C	240
C120	10	C-RF	42 °C	120
C240	10	C-RF	42 °C	240

N: Number; Tem: Temperature.

Material and Methods

Groups of the Animal and RF Procedure

This study was carried out in cooperation with the Department of Anesthesiology and Reanimation and the Department of Histology and Embryology at Akdeniz University. The study was approved by the Animal Studies Ethics Committee of Akdeniz University (TTU-2016-1672).

60 female Rattus Norvegicus rats were used for this study. All rats were healthy before the experiment. For general anesthesia, 0.15 mg/kg bw (body weight) ketamine hydrochloride and 0.02 mg/kg bw 2% Xylazine hydrochloride were injected intraperitoneally into the rats. Then the rats were placed in a prone position, shaved in the abdominal and gluteal regions, and these regions were sterilized using a povidone-iodine solution. A neutral electrode of the radiofrequency device was placed in the abdominal region. The sciatic nerve was exposed by a surgical incision using 22 G, 5 mm RF electrodes. These electrodes were placed without damaging the nerves. When the impedance level was measured between 300–700 ohm, electrical stimulation was given and motor activity was observed. Rats were divided into six groups (Table 1) according to the duration and methods of electrical stimulation:

1. Control (n:10) - Only dissection was made, no other process
2. Sham (n:10) - RF electrode was placed on the sciatic nerve, no other process
3. P120 (n:10) - RF electrode was placed on the sciatic nerve and P-RF was applied for 120 seconds (sec)/42 °C
4. P240 (n:10) - RF electrode was placed on the sci-

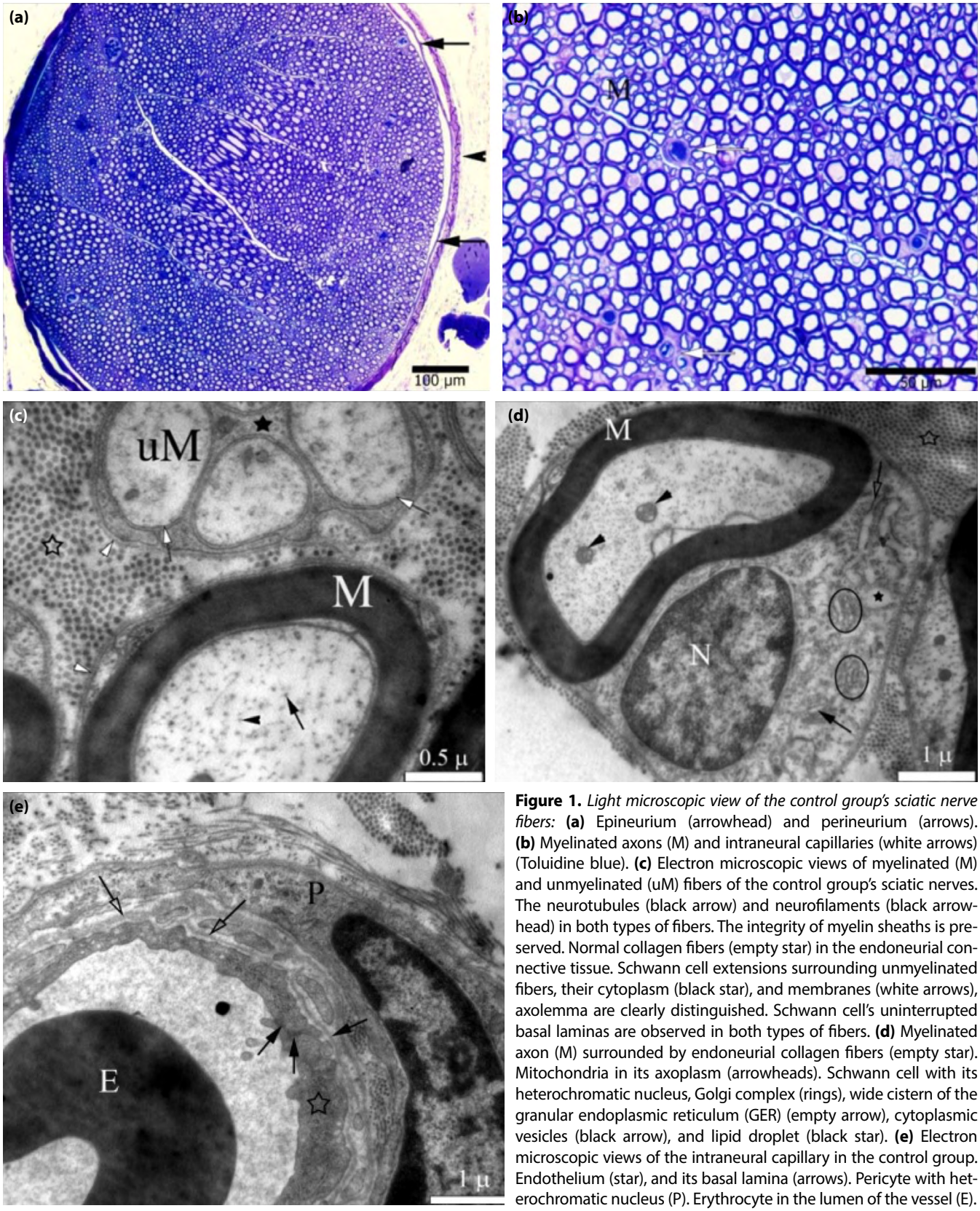

Figure 1. *Light microscopic view of the control group's sciatic nerve fibers:* **(a)** Epineurium (arrowhead) and perineurium (arrows). **(b)** Myelinated axons (M) and intraneural capillaries (white arrows) (Toluidine blue). **(c)** Electron microscopic views of myelinated (M) and unmyelinated (uM) fibers of the control group's sciatic nerves. The neurotubules (black arrow) and neurofilaments (black arrowhead) in both types of fibers. The integrity of myelin sheaths is preserved. Normal collagen fibers (empty star) in the endoneurial connective tissue. Schwann cell extensions surrounding unmyelinated fibers, their cytoplasm (black star), and membranes (white arrows), axolemma are clearly distinguished. Schwann cell's uninterrupted basal laminas are observed in both types of fibers. **(d)** Myelinated axon (M) surrounded by endoneurial collagen fibers (empty star). Mitochondria in its axoplasm (arrowheads). Schwann cell with its heterochromatic nucleus, Golgi complex (rings), wide cistern of the granular endoplasmic reticulum (GER) (empty arrow), cytoplasmic vesicles (black arrow), and lipid droplet (black star). **(e)** Electron microscopic views of the intraneural capillary in the control group. Endothelium (star), and its basal lamina (arrows). Pericyte with heterochromatic nucleus (P). Erythrocyte in the lumen of the vessel (E).

atic nerve and P-RF was applied for 240 sec/42 °C

5. C120 (n:10) - RF electrode was placed on the sciatic nerve and C-RF was applied for 120 sec/42 °C
6. C240 (n:10) - RF electrode was placed on the sciatic nerve and C-RF was applied for 240 sec/42 °C

Rats were kept alive for 48 hours after the experiment. None of them had wound infections or complications for 48 hours. After 48 hours, the sciatic nerves were dissected and 1 cm long samples were taken.

Light and Electron Microscopy

After the cardiac perfusion, tissues from the sciatic nerve were fixed in 4% glutaraldehyde solution (prepared with 0.1 M phosphate buffer - PBS) at +4 °C overnight. Tissues were rinsed with 0.1 M PBS and post-fixed with 1% osmium tetroxide (prepared with 0.1 M PBS) solution at +4 °C for 1 hour. Tissues were rinsed again with 0.1 M PBS and dehydrated with a graded series of ethyl alcohol (30%, 50%, 70%, 80%, 90%, 99%). Then, propylene oxide was applied. The tissues embedded in the Araldite mixture (Araldite CY 212 20 ml, DDSA 22 ml, BDMA 1.1 ml, Dibutyl phthalate 0.5 ml) were held at 60 °C for 48 hours for polymerization. Blocks were cut into semi-thin sections and observed under light microscopy with toluidine blue. Additionally, the blocks were cut into semi-thin and ultra-thin sections using an ultramicrotome. These sections were contrasted with uranyl acetate/lead citrate and observed in a Transmission Electron Microscope (TEM-Zeiss). Myelin damage and degenerative changes were examined in both TEM and light microscopy.

RESULTS

The tissue samples were examined in TEM and light microscopy. In light microscopy, connective tissue sheaths of nerves and leukocyte infiltration into sheaths/nerves were evaluated. Myelinated and unmyelinated axons, Schwann cells, and vessels of nerves were assessed in TEM.

Histological Evidence

Control

No process was applied to the control groups. In light microscopy, there was no change in the histology of nerve fibers (Fig. 1a, b). Nerve fibers and myelin sheaths exhibited normal morphology. Neurotubules and neurofilaments, which are located in axoplasm, were observed to have a normal structure in electron microscopy. The integrity of myelin sheaths and collagens in the endoneurial connective tissues appeared normal. Schwann cell extensions surrounding unmyelinated fibers, as well as their cytoplasm and membranes, axolemma, were distinguishable. Schwann cells' uninterrupted basal laminas were observed in both types of fibers (Fig. 1c, d).

In the investigation of intraneural vessel structure, the unity of endothelial cells and pericytes, the integrity of their basal lamina, and tight junctions were observed to be normal. No leukocytes were observed around the vessels or in the endoneurium (Fig. 1e).

Sham

An RF electrode was placed on the sciatic nerve of sham rats, but no other process was done. The Sham group was compared to the control group. In the sham group, sciatic nerve structures were observed to be similar to the control group. Neurotubules, neurofilaments, mitochondria, and vesicles exhibited similar morphology in both types of fibers (Fig. 2a–d). Evaluations of endoneurial vessel structures were the same as the control group as well (Fig. 2e).

P120

An RF electrode was placed onto the sciatic nerve and P-RF was applied for 120 sec. No change was observed in the P120 group's sciatic nerve morphology. Structures were similar to the control. Neurotubules and neurofilaments, mitochondria, and vesicles were normal, as in the control. Myelin sheaths maintained their integrity. There was no swelling or impairment in the inner and outer mesaxons. In Schwann cells, organelles, the heterochromatic nucleus, cisterns of GER, and vesicles of SER, as well as Golgi complexes, were observed as normal in both myelinated and unmyelinated fibers (Fig. 3a–d). In the intraneural vessel structure investigations, endothelial cells and pericyte, the unity of their basal lamina, and tight junctions were observed as normal. No leukocyte was observed around the vessel or in the endoneurium (Fig. 3e).

P240

An RF electrode was placed onto the sciatic nerve and P-RF was applied for 240 sec. Myelin sheath deformations, axoplasm lysis, and electron-dense material deposits were rarely observed in this group. When all samples were examined, these abnormalities were evaluated as negligible abnormalities (Fig. 4a–e). In the intraneural vessel structure investigations, endothelial cells and pericyte, the unity of their basal lamina, and tight junctions were observed as normal. No leukocyte was observed around the vessel or in the endoneurium (Fig. 4f).

C120

An RF electrode was placed onto the sciatic nerve and C-RF was applied for 120 sec. In the C120

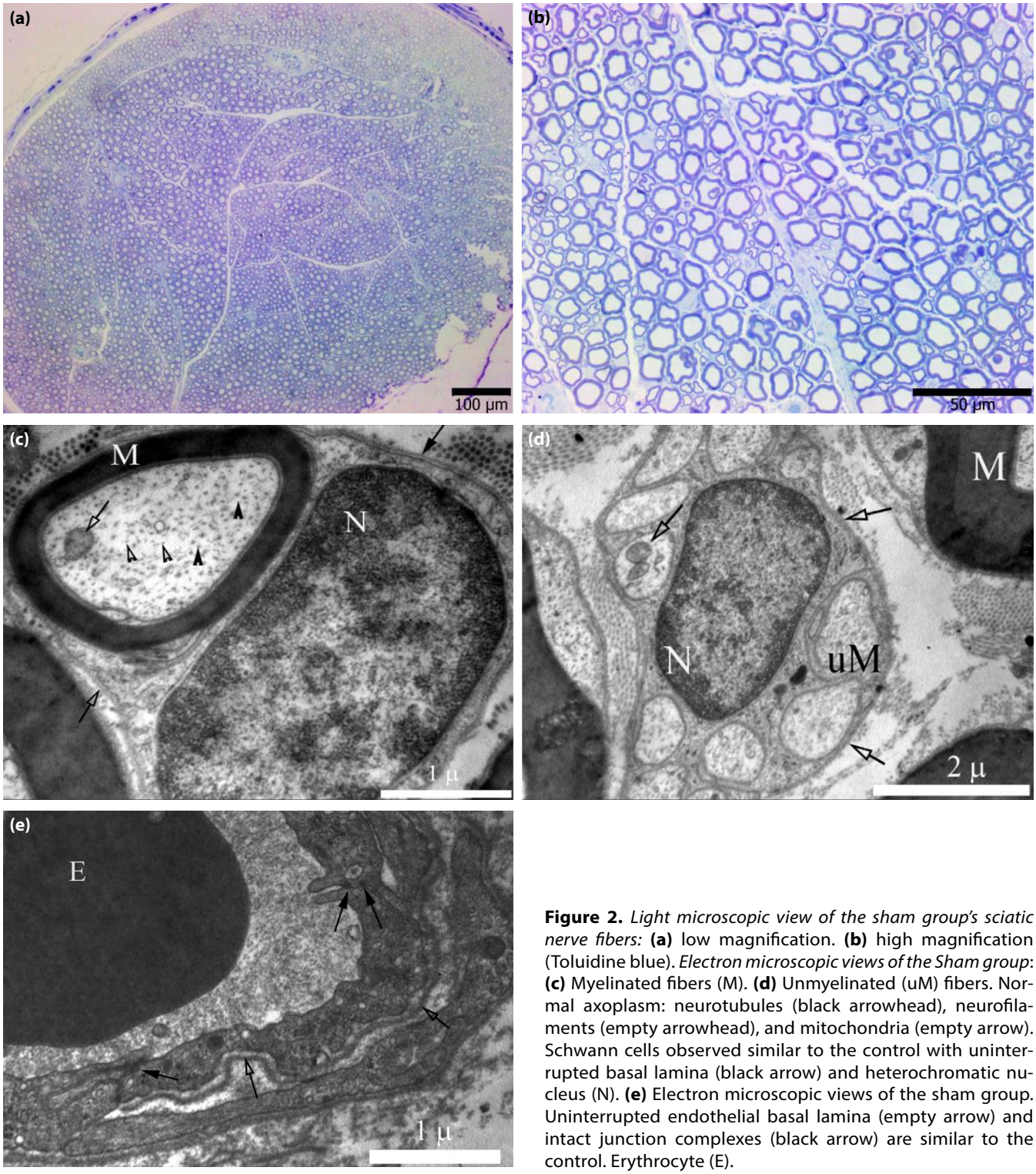

Figure 2. *Light microscopic view of the sham group's sciatic nerve fibers:* **(a)** low magnification. **(b)** high magnification (Toluidine blue). *Electron microscopic views of the Sham group*: **(c)** Myelinated fibers (M). **(d)** Unmyelinated (uM) fibers. Normal axoplasm: neurotubules (black arrowhead), neurofilaments (empty arrowhead), and mitochondria (empty arrow). Schwann cells observed similar to the control with uninterrupted basal lamina (black arrow) and heterochromatic nucleus (N). **(e)** Electron microscopic views of the sham group. Uninterrupted endothelial basal lamina (empty arrow) and intact junction complexes (black arrow) are similar to the control. Erythrocyte (E).

group, there were no structural abnormalities observed in both TEM and light microscopy. Views were similar to the control group (Fig. 5a–d). Neurotubules and neurofilaments, mitochondria, and vesicles were normal, as in the control. The integrity of myelin sheaths was maintained. There was no swelling or impairment in the inner and outer mesaxons. In Schwann cells, organelles such as the heterochromatic nucleus, cisterns of GER, vesicles of SER, and Golgi complexes were observed to be normal in both myelinated and unmyelinated fibers.

In the intraneural vessel structure investigations, endothelial cells and pericytes, the integrity of their basal lamina, and tight junctions were observed as normal. No leukocytes were observed around the vessel or in the endoneurium (Fig. 5e).

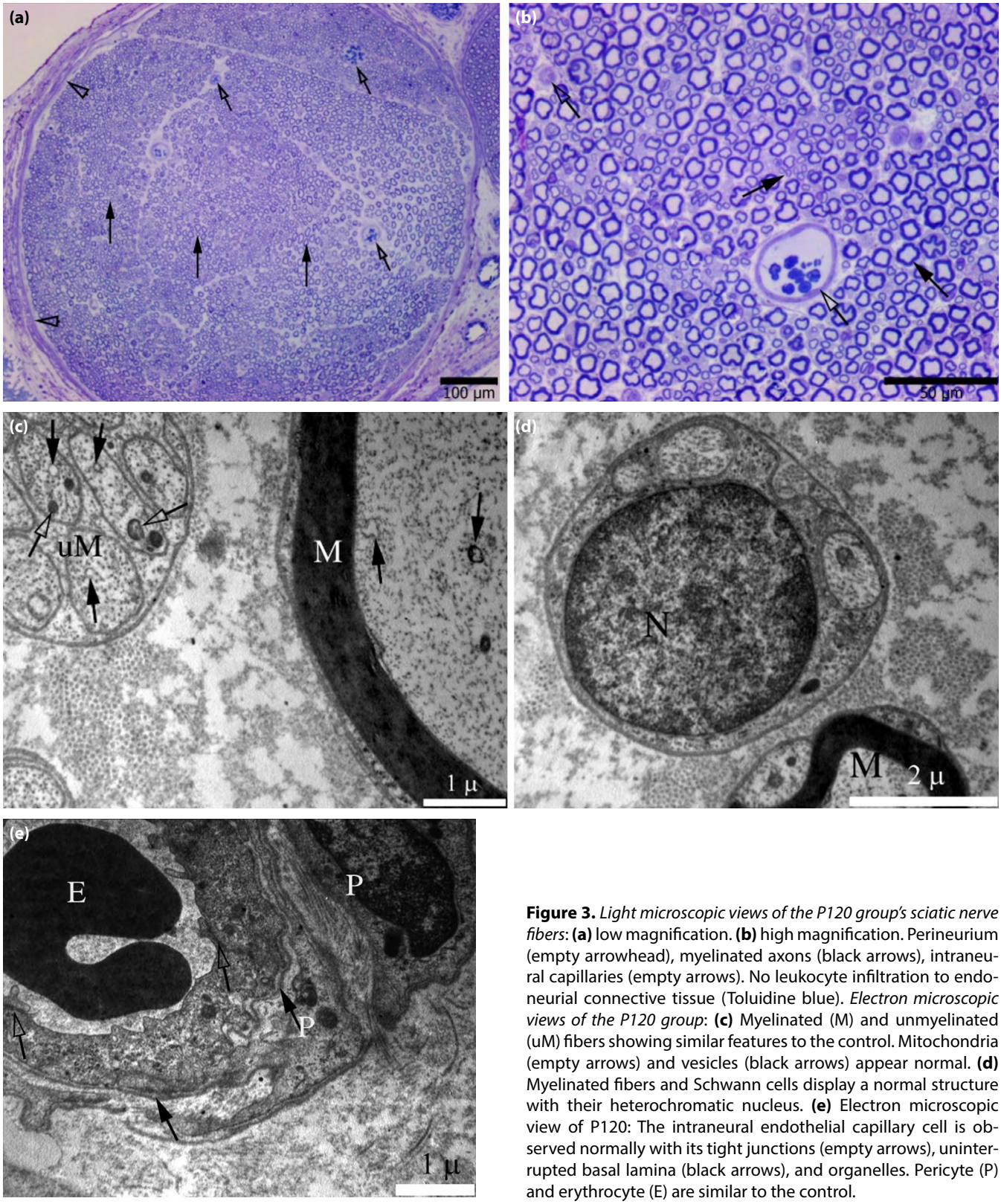

Figure 3. *Light microscopic views of the P120 group's sciatic nerve fibers*: **(a)** low magnification. **(b)** high magnification. Perineurium (empty arrowhead), myelinated axons (black arrows), intraneural capillaries (empty arrows). No leukocyte infiltration to endoneurial connective tissue (Toluidine blue). *Electron microscopic views of the P120 group*: **(c)** Myelinated (M) and unmyelinated (uM) fibers showing similar features to the control. Mitochondria (empty arrows) and vesicles (black arrows) appear normal. **(d)** Myelinated fibers and Schwann cells display a normal structure with their heterochromatic nucleus. **(e)** Electron microscopic view of P120: The intraneural endothelial capillary cell is observed normally with its tight junctions (empty arrows), uninterrupted basal lamina (black arrows), and organelles. Pericyte (P) and erythrocyte (E) are similar to the control.

C240

An RF electrode was placed onto the sciatic nerve and C-RF was applied for 240 sec. Intense deformations were observed in both myelinated and unmyelinated axons. These deformations were characterized as myelin sheath lysis, separation in layers, axoplasmic lysis, loss of axoplasm, loss of mesaxons, and residues of myelin. Many axons showed loss of neurotubules and neurofilaments, loss of mitochondrial cristae, or shrinkage. Dramatic structural disruptions were observed in Schwann cells, including loss of basal lamina, disruption of

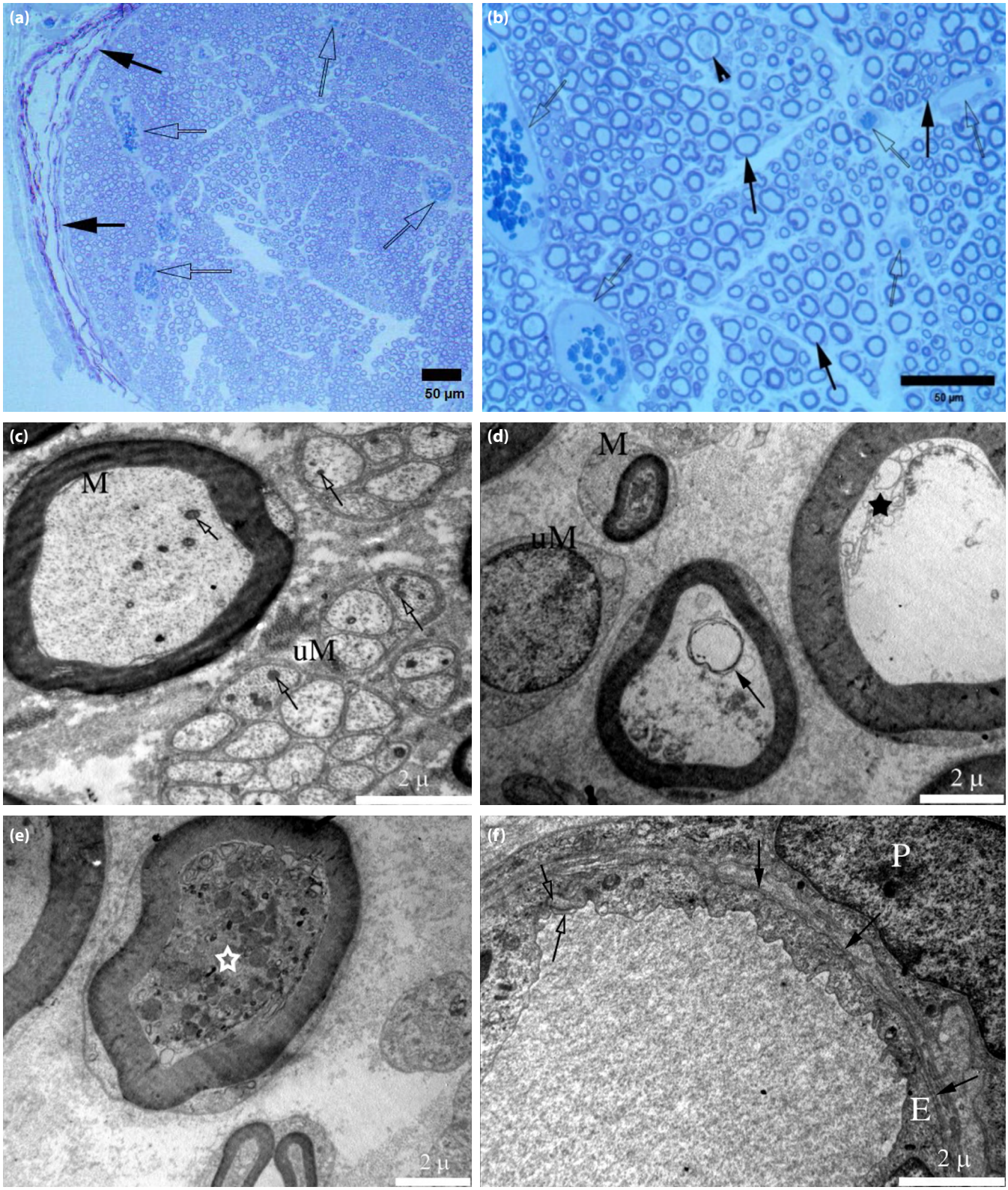

Figure 4. *Light microscopic views of the P240 group*: **(a)** At low magnification, the perineurium (black arrows) appears normal, while the epineurium outside the perineurium appears divided due to a technical error. **(b)** At high magnification, intraneural vessels and myelinated axons seem to be in a normal structure. Also, instances of axonal shrinkage are observed (arrowhead). Neutrophil infiltration is not observed in the endoneurial connective tissue (Toluidine blue). *Electron microscopic view of P240:* **(c)** Myelinated (M) and unmyelinated (uM) axons, and mitochondria (empty arrow) are observed normally. **(d, e)** Structural deformations are observed in some myelinated axons (stars). In these fibers, the myelin sheath is normal, but axoplasm has abnormal morphology. **(d)** Neurofilament and neurotubule structures of some axons are lost, and in some fibers, axoplasmic vesicles swell abnormally and their structure is disrupted (arrow). **(f)** In an axon, axoplasm is full of compact ingredients and has undefined electron-dense material. *Electron microscopic view of P240*: Capillary endothelium (E), tight junction complexes (empty arrows), basal lamina of the endothelium (black arrows), and pericyte appear normal.

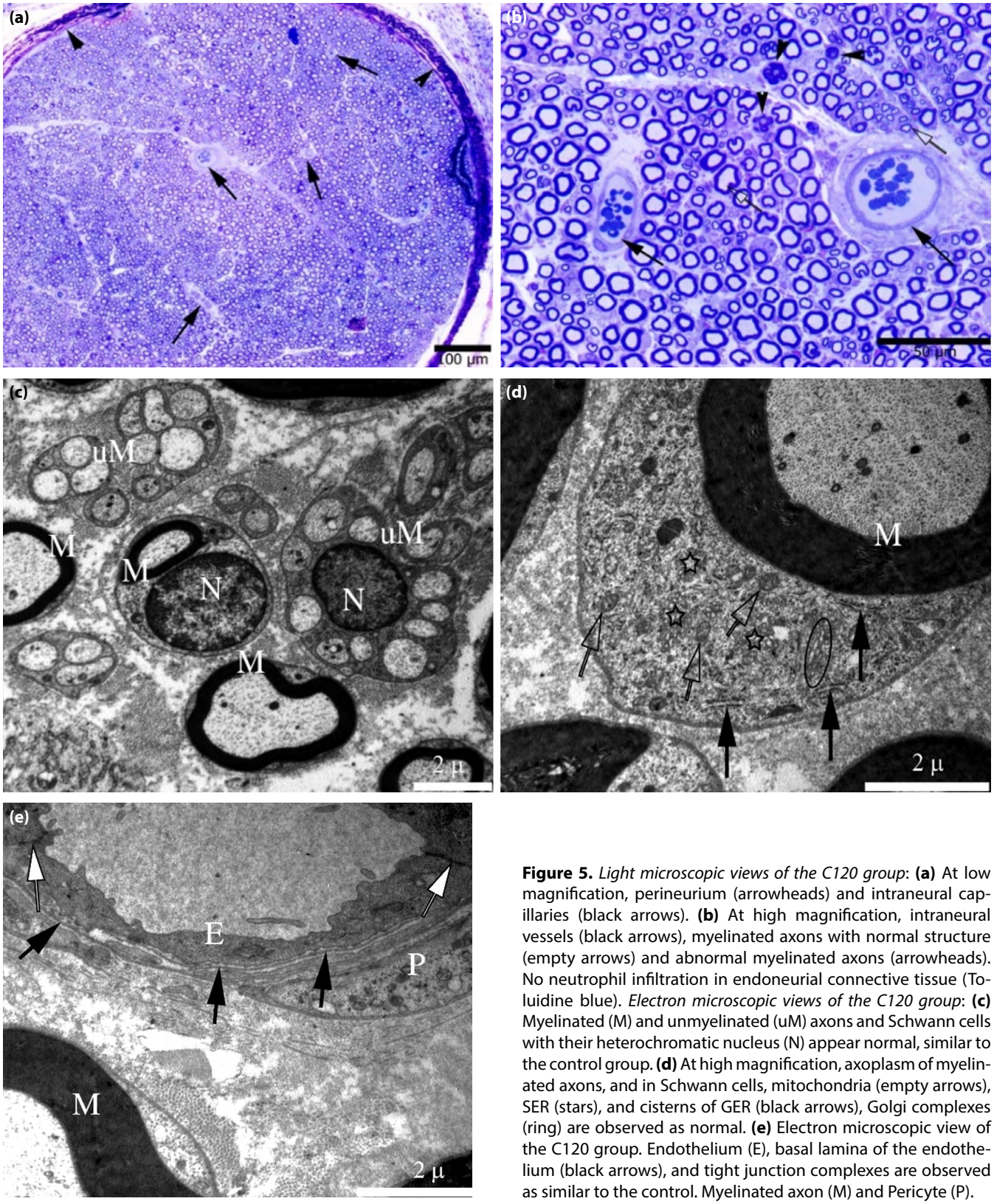

Figure 5. *Light microscopic views of the C120 group*: **(a)** At low magnification, perineurium (arrowheads) and intraneural capillaries (black arrows). **(b)** At high magnification, intraneural vessels (black arrows), myelinated axons with normal structure (empty arrows) and abnormal myelinated axons (arrowheads). No neutrophil infiltration in endoneurial connective tissue (Toluidine blue). *Electron microscopic views of the C120 group*: **(c)** Myelinated (M) and unmyelinated (uM) axons and Schwann cells with their heterochromatic nucleus (N) appear normal, similar to the control group. **(d)** At high magnification, axoplasm of myelinated axons, and in Schwann cells, mitochondria (empty arrows), SER (stars), and cisterns of GER (black arrows), Golgi complexes (ring) are observed as normal. **(e)** Electron microscopic view of the C120 group. Endothelium (E), basal lamina of the endothelium (black arrows), and tight junction complexes are observed as similar to the control. Myelinated axon (M) and Pericyte (P).

membrane integrity, disintegration of cytoplasm into the endoneurium, and loss of heterochromatic appearance due to increased electron density in the nucleoplasm (Fig. 6a–f).

In the intraneural vessel structure investigations, endothelial cells and pericytes, the integrity of their basal lamina, and tight junctions were observed to be normal. Only mitochondrial crista lysis was observed in these two types of cells. No leukocytes were observed around the vessel or in the endoneurium (Fig. 6g).

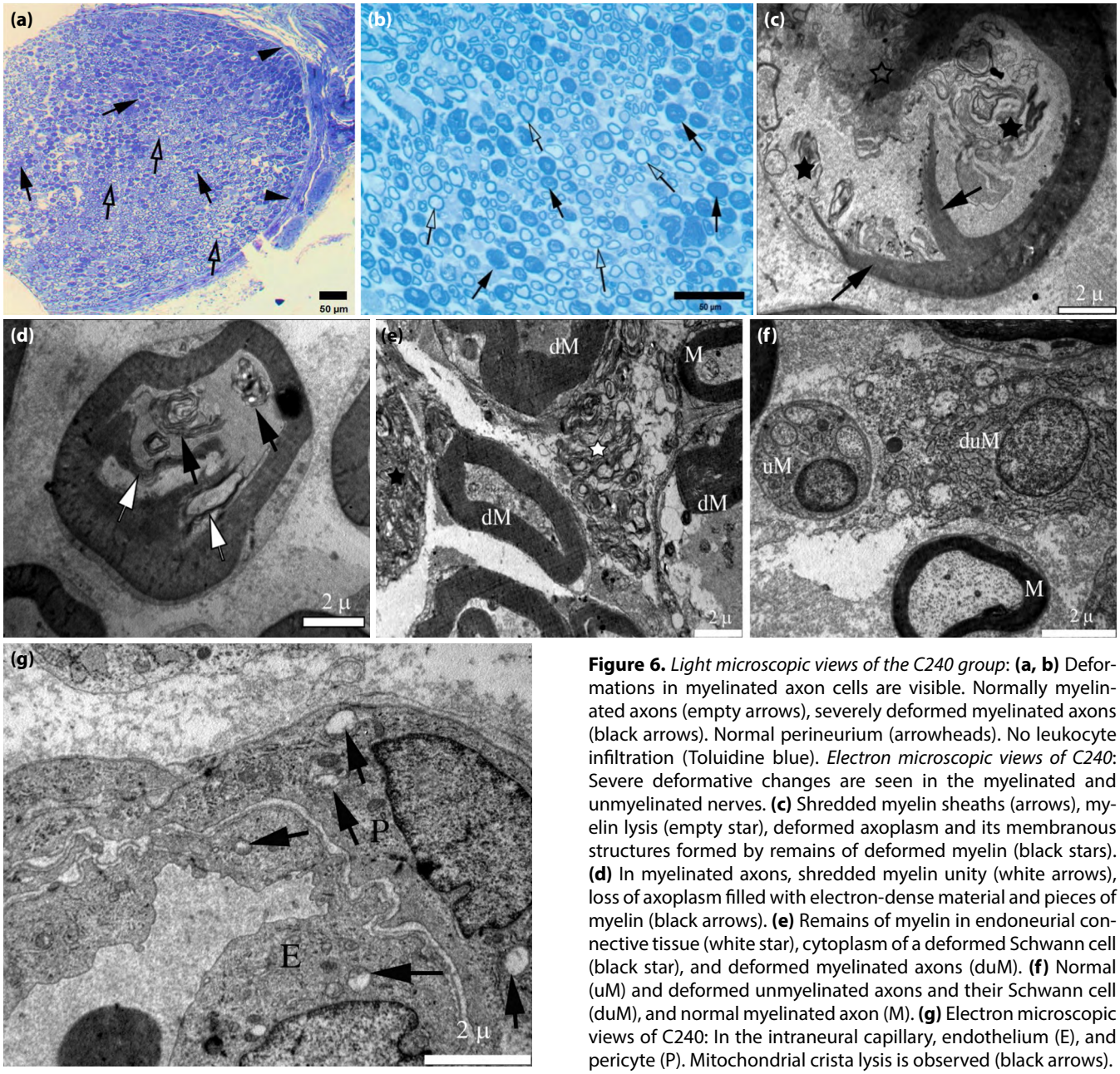

Figure 6. *Light microscopic views of the C240 group*: **(a, b)** Deformations in myelinated axon cells are visible. Normally myelinated axons (empty arrows), severely deformed myelinated axons (black arrows). Normal perineurium (arrowheads). No leukocyte infiltration (Toluidine blue). *Electron microscopic views of C240*: Severe deformative changes are seen in the myelinated and unmyelinated nerves. **(c)** Shredded myelin sheaths (arrows), myelin lysis (empty star), deformed axoplasm and its membranous structures formed by remains of deformed myelin (black stars). **(d)** In myelinated axons, shredded myelin unity (white arrows), loss of axoplasm filled with electron-dense material and pieces of myelin (black arrows). **(e)** Remains of myelin in endoneurial connective tissue (white star), cytoplasm of a deformed Schwann cell (black star), and deformed myelinated axons (duM). **(f)** Normal (uM) and deformed unmyelinated axons and their Schwann cell (duM), and normal myelinated axon (M). **(g)** Electron microscopic views of C240: In the intraneural capillary, endothelium (E), and pericyte (P). Mitochondrial crista lysis is observed (black arrows).

Discussion

Most people develop severe pain due to various nervous or musculoskeletal pathologies. Pain control is very important as it significantly impacts the quality of life of patients. Corticosteroids, frequently used for pain control, have various side effects. Electrical stimulation is known to have a pain-reducing effect similar to corticosteroid injections. C-RF and P-RF are electrical stimulations often used to alleviate pain.[17]

RF technology has been used for many years to interrupt pain conduction. Initially, the pain-relieving effects of RF were attributed solely to thermocoagulation due to blocking C and small delta fibers. However, subsequent research suggested another pain-relieving mechanism. RF can generate an electromagnetic field, which can alleviate pain. Additionally, an electromagnetic field is thought to cause fewer side effects compared to thermocoagulation. In the older technique (C-RF), RF cannot create a sufficient electromagnetic field and has many different side effects. Therefore, a new technique, P-RF, was introduced.[18] P-RF is a painless and nondestructive technique with fewer side effects. It can create biological effects due to rapidly changing electrical fields.[19]

Nerve tissue can be damaged in various ways, such as mechanical, thermal, electromagnetic fields, electrical, etc. In different studies, researchers have

emphasized the importance of avoiding damage from sources other than electromagnetic fields to understand the real effects of the electromagnetic field on nerve tissue. Uematsu and Smith et al.[20] found that RF can damage both small and large nerves, with both myelinated and unmyelinated nerves being damaged at different temperatures.[7] However, de Louw et al.[21] observed no changes in light microscopy due to C-RF in goats and suggested that Smith and Lecher's results might be due to the placement of electrodes in neural tissue and the use of large electrodes. It is crucial to differentiate between mechanical damage and RF damage. For this purpose, we used modern small electrodes and created both sham and control groups. Additionally, we placed electrodes beside the sciatic nerve to minimize mechanical damage. The lack of morphological changes between the control and sham groups indicates that we managed to reduce mechanical damage to a minimum.

C-RF Groups

C-RF exposes target nerves or tissues to continuous electrical stimulation, increasing the temperature and thereby damaging the structures.[22] Both short-term and long-term conventional radiofrequency applied to patients with lumbar facet joint pain for medial branch neurolysis have been shown to positively affect the quality of life and daily activities of the patients.[23]

In a study, dorsal root ganglia and sciatic nerves of rats were exposed to C-RF at 42 °C for 120 sec. Researchers found no significant histopathological effects, except for edema, due to this application. However, at 80 °C, the C-RF application process led to necrosis.[16] For rabbits, C-RF was applied to dorsal root ganglia for 60 sec at 67 °C, resulting in some mitochondrial, nuclear membranal, and neurolemmal changes.[13] de Louw et al.[21] applied C-RF to goat dorsal root ganglia for 60 sec at 67 °C. They did not examine electron microscopy and found no histological changes in light microscopy, but they did observe increased MIB-1 activity, an indirect marker of damage, in the RF group. In Choi et al.'s[24] study, P-RF was applied to rats' sciatic nerves for 60 sec at 80 °C, showing severely degenerated and stunted myelinated axons in the C-RF group.

Vatansever et al.[14] applied C-RF at 40 °C and 80 °C for 90 sec to rats, observing endoneurial and perineural edema in light microscopy and some morphological changes in electron microscopy in the 40 °C group, with these effects intensifying in the 80 °C group. Tun et al.[15] applied RF to rats at 42 °C for 120 sec and 70 °C for 60 sec, noting significant damage, loss of cytoskeleton, Wallerian degeneration, and mitochondrial swelling. Unmyelinated fibers were evaluated as normal.

As mentioned above, there are varied results regarding C-RF's effects on nerve fibers. These studies were conducted on different animals and tissues, with different application periods and techniques. In our study, C-RF was applied for 120 and 240 sec at 42 °C. We found that nerve damage in C-RF groups is related to the duration of application. In the C240 group, intense deformation in myelinated and unmyelinated fibers was observed. However, in the C120 group, myelinated and unmyelinated fibers appeared normal, similar to Podhajski's study, except for reversible edema.[16] Erdine et al.[13] and de Louw applied higher temperatures and shorter durations on different animals than in our study, so their results may be related to the different application temperatures and the use of different animals.[21] In human peripheral nerves, it has been shown that C-RF can cause mitochondrial changes and lead to apoptosis.[25] We did not detect significant changes in light microscopy or electron microscopy in the C120 group. Thus, our study differs from Vatansever's study, and we only observed similar results to Tun's study in the C240 group, not in the C120 group.

P-RF Groups

P-RF, known for its pain-reducing effect similar to corticosteroids but without serious side effects, is preferred in the treatment of various types of pain.[17] P-RF treatment applied to elderly patients with postherpetic neuralgia has been shown to be safe and effective.[26] It has also been reported that intradiscal P-RF application can be an effective and safe technique in the treatment of chronic discogenic neck pain.[27]

Erdine et al.[13] applied P-RF to rabbit dorsal root ganglia for 120 sec at 42 °C. They observed enlargement

of ER cisterns and vacuole groups, with no pathological changes in cell membranes or nerve fibers' morphology. Another study found that P-RF could cause more damage than control groups and that C fibers were particularly affected.[28]

In a study with rats exposed to P-RF for 120 sec at 42 °C, cytoplasmic vacuoles, expansion of ER cisterns, mitochondrial damage, nuclear and plasma membrane damage, and some changes in Schwann cells were observed in myelinated fibers.[29] Choi et al.[24] also applied P-RF to rats' sciatic nerves for 120 sec at 42 °C, finding some myelinated axon damage and swelling. Vatansever et al.,[14] applying P-RF for 240 sec at 42 °C, determined some nerve damage. These results differ from our study. In our study, no significant morphological or pathological changes were observed in both P-RF groups, except for some negligible abnormalities in the 240 sec P-RF group, such as myelin sheath deformations, axoplasmic lysis, and electron-dense material deposits.

Another research observed normal morphology in both myelinated and unmyelinated nerves, except for a few axons where myelin separated, and newly formed myelin sheaths were noticed.[15] Podhanjski et al.,[16] applying P-RF for 120 sec at 42 °C to rats, observed reversible edema in dorsal root cells and sciatic nerves, with no other abnormalities. It has been shown that P-RF does not cause morphological changes in mitochondria or induce apoptosis in human peripheral nerves.[25] Several studies demonstrate that P-RF can have a positive histological effect on damaged nerves. Zhu et al.[30] demonstrated that P-RF can promote nerve repair by increasing the level of GDNF and decreasing the level of GFAP. P-RF can be applied at different voltage levels, causing different morphological changes in nerves. High voltage P-RF in rat's sciatic nerves can down-regulate Nav 1.7, induce histological changes, and improve pain more effectively than other levels.[31] Preliminary research suggests that P-RF can lead to nerve regrowth and decrease nerve damage.[32]

These results align with our findings in the P120 group, but we did not observe newly formed myelin sheaths or edema.

Conclusion

In our study, we demonstrated that the application of P-RF for both 120 sec and 240 sec, as well as C-RF for 120 sec at 42 °C, did not induce any deformations in rats' sciatic nerves. However, the application of C-RF for 240 sec at the same temperature caused pathological changes in the nerves. Thus, it can be inferred that damage may increase with the extension of the duration of the experiment. While some studies support our findings, numerous other studies have reported contradictory results. Additionally, it has been suggested that P-RF can promote nerve repair.

It is evident that there is no consensus on the morphological and pathological effects of RF on nerves. Despite the frequent use of these treatment modalities in daily clinical practice, the underlying mechanisms of PRF and CRF are not yet fully understood. Further research is necessary to comprehend these mechanisms and ascertain their specific morphological effects.

Ethical Approval: The Akdeniz University Animal Studies Ethics Committee granted approval for this study (date: 11.04.2016, number: TTU-2016-1672).

Conflict-of-interest issues regarding the authorship or article: None declared.

Financial Disclosure: This work was supported by the Scientific Research Projects Coordination Unit (BAP) (TTU-2016-1672) of Akdeniz University.

Peer-rewiew: Externally peer-reviewed.

References

1. Pain terms: A list with definitions and notes on usage. Recommended by the IASP subcommittee on taxonomy. Pain 1979;6:249.
2. Hylands-White N, Duarte RV, Raphael JH. An overview of treatment approaches for chronic pain management. Rheumatol Int 2017;37:29–42. [CrossRef]
3. Smith H, Youn Y, Guay RC, Laufer A, Pilitsis JG. The role of invasive pain management modalities in the treatment of chronic pain. Med Clin North Am 2016;100:103–15. [CrossRef]
4. Sun HH, Zhuang SY, Hong X, Xie XH, Zhu L, Wu XT. The efficacy and safety of using cooled radiofrequency in treating chronic sacroiliac joint pain: A PRISMA-compliant meta-analysis. Medicine (Baltimore) 2018;97:e9809. [CrossRef]
5. Sweet WH, Wepsic JG. Controlled thermocoagulation of trigeminal ganglion and rootlets for differential destruction of pain fibers. 1. Trigeminal neuralgia. J Neurosurg 1974;40:143–56. [CrossRef]

6. Rosomoff HL, Brown CJ, Sheptak P. Percutaneous radiofrequency cervical cordotomy: Technique. J Neurosurg 1965;23:639–44. [CrossRef]
7. Uematsu S. Percutaneus electrothermocoagulation of spinal nevre trunk, ganglion and rootlets. In: Schmidel H, Sweet WH, editors. Current Techique in Operative Neurosurgery. New York: Grune and Stratton; 1977. p.469–90.
8. Shealy CN. Percutaneous radiofrequency denervation of spinal facets. Treatment for chronic back pain and sciatica. J Neurosurg 1975;43:448–51. [CrossRef]
9. Lord SM, Bogduk N. Radiofrequency procedures in chronic pain. Best Pract Res Clin Anaesthesiol 2002;16:597–617.
10. Choi EJ, Choi YM, Jang EJ, Kim JY, Kim TK, Kim KH. Neural ablation and regeneration in pain practice. Korean J Pain 2016;29:3–11. [CrossRef]
11. Chua NH, Vissers KC, Sluijter ME. Pulsed radiofrequency treatment in interventional pain management: Mechanisms and potential indications-a review. Acta Neurochir (Wien) 2011;153:763–71. [CrossRef]
12. Racz GB, Ruiz-Lopez R. Radiofrequency procedures. Pain Pract 2006;6:46–50. [CrossRef]
13. Erdine S, Yucel A, Cimen A, Aydin S, Sav A, Bilir A. Effects of pulsed versus conventional radiofrequency current on rabbit dorsal root ganglion morphology. Eur J Pain 2005;9:251–6. [CrossRef]
14. Vatansever D, Tekin I, Tuglu I, Erbuyun K, Ok G. A comparison of the neuroablative effects of conventional and pulsed radiofrequency techniques. Clin J Pain 2008;24:717–24.
15. Tun K, Cemil B, Gurcay AG, Kaptanoglu E, Sargon MF, Tekdemir I, et al. Ultrastructural evaluation of Pulsed Radiofrequency and Conventional Radiofrequency lesions in rat sciatic nerve. Surg Neurol 2009;72:496–501. [CrossRef]
16. Podhajsky RJ, Sekiguchi Y, Kikuchi S, Myers RR. The histologic effects of pulsed and continuous radiofrequency lesions at 42 degrees C to rat dorsal root ganglion and sciatic nerve. Spine (Phila Pa 1976) 2005;30:1008–13. [CrossRef]
17. Park D, Chang MC. The mechanism of action of pulsed radiofrequency in reducing pain: A narrative review. J Yeungnam Med Sci 2022;39:200–5. [CrossRef]
18. Sluitjer ME. The effects of pulsed radiofrequency fields applied to the dorsal root ganglion: A preliminary report. Pain Clin 1998;11:109–17.
19. Sluijter EM, van Kleef M. Characteristics and mode of action of radiofrequency lesions. Curr Rev Pain 1998;2:143–50.
20. Smith HP, McWhorter JM, Challa VR. Radiofrequency neurolysis in a clinical model. Neuropathological correlation. J Neurosurg 1981;55:246–53. [CrossRef]
21. de Louw AJ, Vles HS, Freling G, Herpers MJ, Arends JW, Kleef M. The morphological effects of a radio frequency lesion adjacent to the dorsal root ganglion (RF-DRG)--an experimental study in the goat. Eur J Pain 2001;5:169–74.
22. Kwak SG, Lee DG, Chang MC. Effectiveness of pulsed radiofrequency treatment on cervical radicular pain: A meta-analysis. Medicine (Baltimore) 2018;97:e11761. [CrossRef]
23. Çetin A, Yektaş A. Evaluation of the short- and long-term effectiveness of pulsed radiofrequency and conventional radiofrequency performed for medial branch block in patients with lumbar facet joint pain. Pain Res Manag 2018;2018:7492753. [CrossRef]
24. Choi S, Choi HJ, Cheong Y, Lim YJ, Park HK. Internal-specific morphological analysis of sciatic nerve fibers in a radiofrequency-induced animal neuropathic pain model. PLoS One 2013;8:e73913. [CrossRef]
25. Nishioka A, Kimura M, Sakamoto E, Nagasaka H, Azma T. Continuous but not pulsed radiofrequency current generated by NeuroTherm NT500 impairs mitochondrial membrane potential in human monocytic cells THP-1. J Pain Res 2020;13:1763–8. [CrossRef]
26. Huang X, Ma Y, Wang W, Guo Y, Xu B, Ma K. Efficacy and safety of pulsed radiofrequency modulation of thoracic dorsal root ganglion or intercostal nerve on postherpetic neuralgia in aged patients: A retrospective study. BMC Neurol 2021;21:233. [CrossRef]
27. Kwak SY, Chang MC. Effect of intradiscal pulsed radiofrequency on refractory chronic discogenic neck pain: A case report. Medicine (Baltimore) 2018;97:e0509. [CrossRef]
28. Erdine S, Bilir A, Cosman ER, Cosman ER Jr. Ultrastructural changes in axons following exposure to pulsed radiofrequency fields. Pain Pract 2009;9:407–17. [CrossRef]
29. Protasoni M, Reguzzoni M, Sangiorgi S, Reverberi C, Borsani E, Rodella LF, et al. Pulsed radiofrequency effects on the lumbar ganglion of the rat dorsal root: A morphological light and transmission electron microscopy study at acute stage. Eur Spine J 2009;18:473–8. [CrossRef]
30. Zhu Q, Yan Y, Zhang D, Luo Q, Jiang C. Effects of pulsed radiofrequency on nerve repair and expressions of GFAP and GDNF in rats with neuropathic pain. Biomed Res Int 2021;2021:9916978. [CrossRef]
31. Dai Z, Xu X, Chen Y, Lin C, Lin F, Liu R. Effects of high-voltage pulsed radiofrequency on the ultrastructure and Nav1.7 level of the dorsal root ganglion in rats with spared nerve injury. Neuromodulation 2022;25:980–8. [CrossRef]
32. Li DY, Meng L, Ji N, Luo F. Effect of pulsed radiofrequency on rat sciatic nerve chronic constriction injury: A preliminary study. Chin Med J (Engl) 2015;128:540–4. [CrossRef]